Optically detected magnetic resonance of the triplet state of copper-center—donor pairs in CdS

J. J. Davies* and R. T. Cox
Section de Résonance Magnétique, Département de Recherche Fondamentale, Centre d'Etudes Nucléaires de Grenoble 85X, 38041 Grenoble-Cedex, France

J. E. Nicholls
Department of Physics, University of Hull, Hull, HU6 7RX, United Kingdom
(Received 30 March 1984)

Eight distinct types of triplet-state optically detected magnetic resonance (ODMR) spectra have been obtained at 2 K by monitoring the intensity of a broad emission band (peak wavelength 720 nm) observed for undoped, vapor-phase CdS crystals. Several of the ODMR spectra show hyperfine structure due to copper. The signals are attributed to exchange-coupled pairs consisting of a shallowly bound electron and a hole that is localized in the $3d$ shell of a copper ion. The copper ion is part of an associate center CuX, which can be oriented either parallel to or at 109° to the crystal c axis. The eight different spectra correspond to different geometrical arrangements of this center and of a nearby donor impurity. Recombination of the electron bound to this complex defect with the copper-center hole gives rise to the optical emission. It is shown how the hyperfine and g tensors for the triplet centers can be related to the corresponding quantities for the individual $S=\frac{1}{2}$ electron and hole centers from which they are constructed.

I. INTRODUCTION

The recombination of electrons from shallow donors with holes from deep acceptors is now recognized to be responsible for many of the broad emission bands observed in II-VI semiconducting materials. Many of these bands have been the subject of optically detected magnetic resonance (ODMR) investigations, and in such experiments it has often been possible to obtain detailed information about the structure of the recombining centers. The ODMR spectra from such systems are usually dominated by contributions from recombining donor-acceptor pairs in which the intrapair separation is large. The donors and acceptors in such pairs are only weakly interacting and two types of ODMR signal are then observed, one due to isolated donors and one due to isolated acceptors (e.g., Refs. 1 and 2).

In contrast, when the distance separating the donor and acceptor is small, so that the interaction is stronger, the donor-acceptor spin-exchange coupling splits the combined spin states and leads, for the case when both donor and acceptor spins are $\frac{1}{2}$, to a singlet and a triplet which are well separated in energy from each other. ODMR signals from the spin-triplet states are expected, the g factor being equal to the mean of the values for the isolated donors and acceptors. This has been demonstrated[3] in ZnS where sharp ODMR lines from strongly coupled shallow-donor—deep-acceptor (A center) pairs were obtained at the mean g value of the donors and A centers.

For even smaller donor-acceptor separations, additional interactions having the form of an anisotropic exchange coupling will produce a zero-field splitting of the three levels of the triplet. The ODMR signal at the average g value will then become a pair of signals whose separation depends on the magnitude of the zero-field splitting and on the direction of the magnetic field. In this paper we report a series of ODMR spectra of this type which we have observed for certain samples of CdS. These ODMR spectra are associated with emission in the visible-red and near-infrared regions and are attributed to the triplet state of very strongly interacting pairs, each consisting of a shallowly bound donor electron and a deeply bound acceptor hole. The observation of hyperfine structure and the values of the g tensor lead us to conclude that the deep acceptors are copper ions complexed with other impurities.

The properties of our ODMR spectra are in some ways similar to those reported for the triplet states of bound excitons in GaSe,[4] GaP,[5] GaS,[6] and SiC.[7] However, the present results are of particular interest because they appear to be the first cases of ODMR triplet-state spectra in semiconductors in which the values of the g tensor and of the hyperfine tensor can be related directly to those of the individual centers from which the pair is composed.

II. EXPERIMENTAL DETAILS

The crystals used for most of the work were cut from a hexagonal prism (~ 6 mm$\times 3$ mm^2) grown by vapor transport in a closed tube by M. Moulin at the Laboratoire Central de Recherches of Thomson CSF, Corbeville, France.[8] The material was not deliberately doped nor did the growth method involve any halogen or other transporting agent. We obtained similar but weaker ODMR spectra from a vapor-phase sample of different origin supplied by us by G. Bastide.[9]

In the ODMR experiments the intensity of the lumines-

cence was monitored with $S20$ response and multialkaline photomultipliers, and, as the magnetic field was swept, microwave-induced changes in intensity were detected with a lock-in system. Most of the experiments were done at Centre d'Etudes Nucléaires (CEN) de Grenoble with an apparatus working at 8.7 GHz. This apparatus was usually operated in a time-resolved mode[10] in which the laser was pulsed and the photomultiplier switched on by a gating pulse after a predetermined delay. A typical pulse sequence is shown later in the inset of Fig. 2: Microwaves were applied during alternate gating pulses and the difference between alternate photomultiplier output pulses was extracted with lock-in detection. This time-resolved technique was not essential in the present work, but was helpful in separating the spectra of centers with differing optical lifetimes or spin-relaxation times. This was achieved simply by changing the repetition rate of the pulse sequence. The parameters of the spin Hamiltonian were cross-checked at 23 GHz with an apparatus at Hull University similar to that described by Nicholls *et al.*;[2] here, the laser excitation was continuous and the microwaves were chopped at about 10 kHz.

In all the experiments the CdS crystals were in direct contact with liquid helium at 2 K; they were mounted on natural-growth faces with the c axis either vertical or in a horizontal plane containing the magnetic field, and could be rotated about the vertical axis. The precision of the orientation setting and measurement was $\pm 3°$. The luminescence was monitored in a direction perpendicular to the magnetic field.

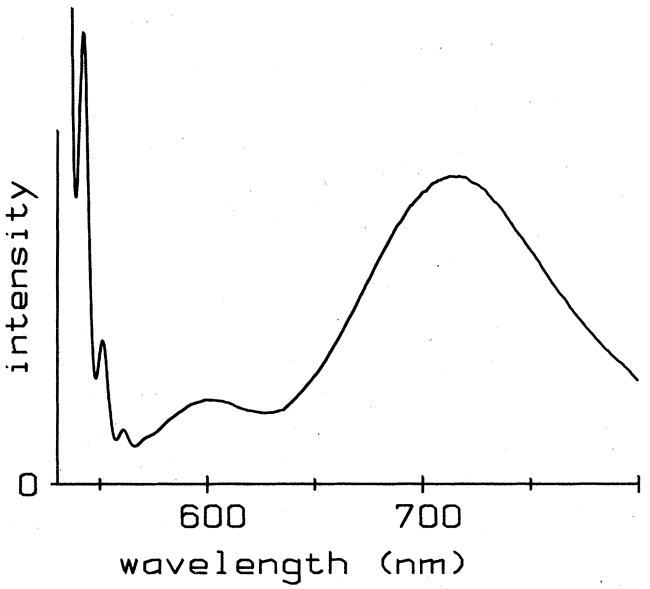

FIG. 1. Emission spectrum from an undoped CdS crystal grown by a vapor-phase method by Moulin. The sample is excited by 488-nm radiation at 2 K. The spectrum has been corrected for instrumental response and is expressed as intensity per unit wavelength interval. The same sample was used for the ODMR spectra of Figs. 2–6, the total emission in the (620–800)-nm region being monitored.

III. OPTICAL SPECTRA

Intense luminescence was obtained under laser excitation at 2 K. A spectrum obtained with 488-nm excitation is shown in Fig. 1. The spectrum contains three main features:

(i) A series of relatively narrow bands at high energy (515–560 nm) that result from the well-known process of shallow-donor—to—shallow-acceptor, distant-pair recombination.[11] These bands have been the subject of previous ODMR studies.[12,13]

(ii) A broad, structureless band in the visible-orange region with a peak wavelength at about 600 nm. This may be the band associated with silver impurities mentioned in the older luminescence literature;[14] it disappears if the laser wavelength is shifted to 514 nm.

(iii) A more intense, broad band in the visible-red—infrared region, peaking at about 720 nm. This band is the subject of the present paper and will be attributed to centers involving copper impurities. A very similar band appears in several published spectra,[15–17] but the association with copper appears not to have been made previously. Instead, deliberate copper doping produces unexplained bands at about 780 and 1000 nm (Ref. 17) (as well as the well-known ^2E-to-$^2T_2$ internal emission of Cu^{2+} in the 1.6-μm region[18]). The band at 720 nm is apparently characteristic of nominally pure CdS crystals grown by the vapor-phase method.[19]

For the 720-nm emission band we have made some studies of the form of the time decay following pulsed laser excitation. The decay curve was very complex, being the sum of many components with lifetimes ranging from less than our minimum measuring time of 1 μs to hundreds of microseconds (the most prominent component had a lifetime of ~ 11 μs). Application of very small magnetic fields (~ 10 mT) strongly reduced the luminescence intensity at long delay times (> 10 μs) and increased the intensity at short times (< 10 μs). These changes may represent shortening of certain radiative decay times by field-induced mixing of triplet and singlet states.

We observed related changes in time-resolved luminescence spectra. These were obtained with laser-pulse repetition rates in the (1–100)-kHz range. Application of magnetic field produced large increases or decreases of the height of the 720-nm band, depending on the laser pulse rate. In the time-resolved spectra, there were also small shifts in the peak wavelength of the visible-red—infrared band with magnetic field as well as with laser pulse rate. These shifts are presumably related to the complex substructure of the optical band that is brought out by the ODMR studies to be described below. We have noted similar field-induced effects on the visible-orange emission band (600 nm), which suggests that it too corresponds to triplet-state emission.

IV. ODMR SPECTRA

Our present results concern only the red and infrared emission (beyond 620 nm), for which we have obtained eight different ODMR spectra. These eight spectra each correspond to an $S=1$ species with its major magnetic

symmetry axis either close to the c axis or close to a direction inclined at 109° to the c axis. ODMR signals can also be obtained from the orange emission near 600 nm, but these will not be discussed in the present paper.

A. Centers with c-axis symmetry

When the red and infrared radiation between 620 and 800 nm is monitored, the ODMR spectrum for the magnetic field along the c axis (Figs. 2–4) is dominated by four types of signals. At 8.7 GHz the four types are as follows:

(i) A pair of strong broad lines at 0.208 and 0.413 T (Fig. 2) showing partly resolved hyperfine structure and of asymmetric shape as shown on an expanded scale for the low-field line in Fig. 3. These signals are designated type I.

(ii) A pair of signals at 0.239 and 0.382 T showing well-resolved four-line hyperfine structure. These lines also are shown in Fig. 2 and are designated type II A. As the pulse repetition rate is reduced, these signals become more prominent relative to the type I, as may be seen by comparing Figs. 4(a) and 4(b) with Fig. 2.

(iii) A pair of signals at 0.248 and 0.374 T also showing well-resolved four-line hyperfine structure. These lines are not prominent in Figs. 2 and 4(a), which were obtained with 488-nm excitation; they are more easily observed [Fig. 4(b)] when the excitation wavelength is changed to 514 nm. We designate them type II B.

(iv) A complex group of lines in the central region of the spectrum, 0.30 to 0.34 T, and labeled c in Fig. 2; the centers responsible for these signals do not have c-axis symmetry and are discussed in Sec. IV B.

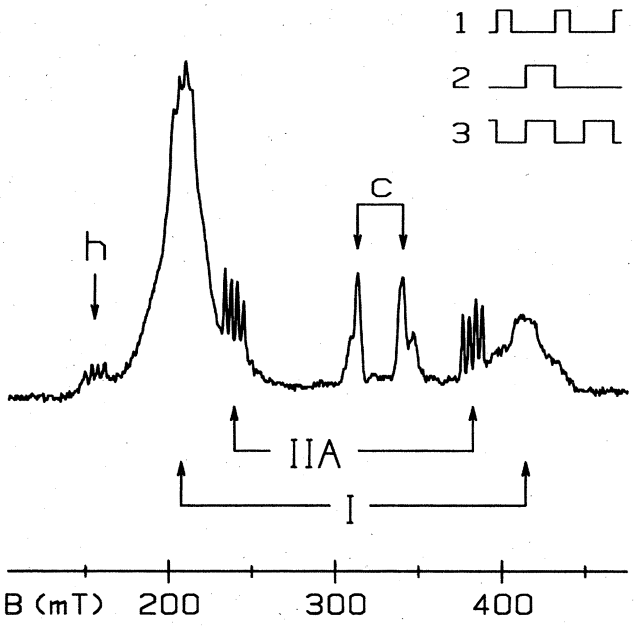

FIG. 2. ODMR spectrum associated with (620–800)-nm emission from the CdS sample excited by 488-nm radiation at 2 K. The microwave frequency was 8.7 GHz and the field was along the crystal c axis. The pulse sequence is shown at top right: 1 denotes laser power, 2 denotes microwave power, and 3 denotes photomultiplier gain; the laser-pulse repetition rate was 25 kHz. The ODMR signal is the difference between alternate photomultiplier output pulses; here and in Figs. 3–8 the upward direction of the vertical axis represents increases in emission intensity with microwaves applied. The lines labeled I and II A, and the central-region lines labeled "c," are discussed in the text; lines "h" are unidentified "half field" ("$\Delta M = \pm 2$") transitions.

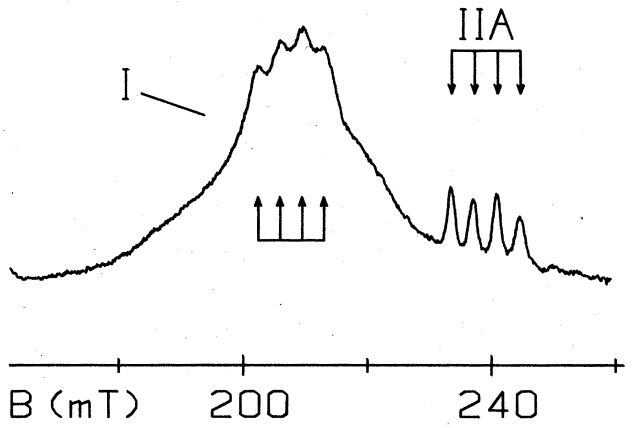

FIG. 3. Expanded recording of the low-field region of the ODMR spectrum of Fig. 2 to show the asymmetric line shape with pronounced shoulders and the hyperfine structure associated with the type-I spectrum.

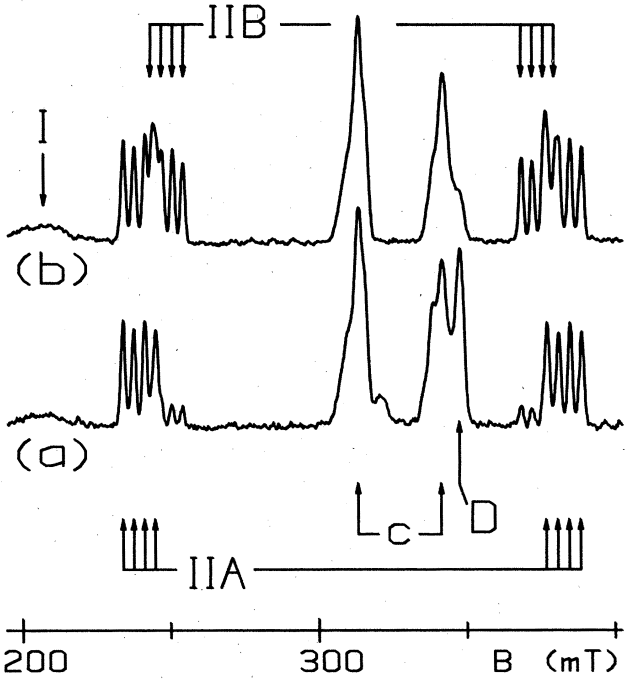

FIG. 4. ODMR spectra at 2 K and 8.7 GHz with the field along the c axis for (a) 488-nm and (b) 514-nm excitation. The pulse sequence was as in Fig. 2, but the laser-pulse rate was reduced to 2.5 kHz, causing the type-I spectrum almost to disappear. Lines II A, II B, and the central-region lines c are discussed in the text; line D is a shallow-donor resonance not studied here.

In the ODMR experiments using cw-laser excitation the optimum signal-to-noise ratios for the type-I, -II A, and -II B spectra were all obtained at the same microwave chopping frequency of 10 kHz. In contrast, in the time-resolved ODMR experiment there was, as noted above, a marked difference in dependence on pulse rate between the different types. A further point is that the type-II A and -II B ODMR spectra can be enhanced by a factor of up to 10 by the application of 100-kHz field modulation of peak-to-peak amplitude 2 mT, while the type-I signals are not enhanced. The effect occurs[20] because the modulation brings into resonance a wide range of the spin packets that make up the inhomogeneously broadened signal, but the degree of enhancement depends on the spin-relaxation times and optical-decay times, which are therefore presumed to be different for the type-I and -II centers.

The type-I, -II A, and -II B spectra correspond to centers having spin $S=1$, the pair of signals in each case corresponding to the allowed microwave transitions $M=0\leftrightarrow M=-1$ and $M=0\leftrightarrow M=+1$, which are separated from each other as a result of the zero-field splitting of the triplet. The type-II A spectrum appears to correspond to exactly cylindrical symmetry about the crystal c axis, while, as discussed below, there is evidence that the type-I and -II B spectra have small additional nonaxial components in the zero-field splitting. We discuss below the details of these three spectra, beginning with type II A, which is the simplest.

1. Type-II A ODMR spectrum

This spectrum can be described by the spin Hamiltonian

$$\mathcal{H}=g_{\|}\beta B_z S_z+g_{\perp}\beta(B_x S_x+B_y S_y)+D[S_z^2-\tfrac{1}{3}S(S+1)] + A_{\|}S_z I_z+A_{\perp}(S_x I_x+S_y I_y)\,, \quad (1)$$

with $S=1$, $I=\frac{3}{2}$, and the z direction along the crystal c axis. The values of the parameters found experimentally are given in Table I; the results obtained at the two microwave frequencies were in excellent agreement. When the c axis is rotated away from the magnetic field direction, the lines gradually become weaker and move in among the central group of signals of Fig. 2. They become unobservable at angles greater than $\sim 40°$, but can be observed again as the field approaches a direction perpendicular to the c axis (see later in Fig. 6). In the perpendicular orientation the hyperfine structure is unresolved and only an upper limit for $|A_{\perp}|$ can be deduced from the observed linewidth.

2. Type-II B ODMR spectrum

At first sight this spectrum is similar to the type-II A spectrum. However, as the magnetic field is rotated away from the c axis, the signals disappear for angles greater than 15°. The signals can again be observed when the field is perpendicular to the c axis (see later in Fig. 6), but, as for the type-II A spectrum, the splitting due to $A_{\perp}$ is not resolved. For this orientation, the type-II B signals are wider than the type-II A signals, and, unlike the type-II A signals, they change shape slightly as the field is rotated in the (0001) plane. These changes are attributed to the presence of small nonaxial components in the zero-field-splitting terms [for example, of form $E(S_x^2-S_y^2)$]. Since the departure from axial symmetry about the c axis is small, we have again used the spin Hamiltonian of Eq. (1), the appropriate parameters being given in Table I.

3. Type-I ODMR spectrum

The behavior of the type-I spectra differs in several respects from that of types II A and II B. For example, the type-I signals are unaffected by the 100-kHz field

TABLE I. Spin-Hamiltonian parameters for the eight $S=1$ ODMR spectra studied in this paper. Measurement precision was generally ±0.001 for g factors, ±1 mT for $D/g_{\|}\beta$, and $\pm 2\times 10^{-4}$ cm^{-1} for $A_{\|}$ (when the hyperfine splitting is resolved). (For the type-III spectrum, poor signal-to-noise ratio prevented meaningful g-factor measurements, and $D/g_{\|}\beta$, measured to ±4 mT, was converted to energy units taking $g_{\|}=2.000$.) The parameters for the centers with z axes at 109° to the c axis are determined in the approximation of cylindrical symmetry about these axes (see text). Parameter λ_{peak} is the emission wavelength that maximizes the ODMR signal. At right, g factors for the copper centers are derived taking $g(\mathrm{Cu})=2g(\mathrm{pair})-g(D)$, where $g(D)$ is the shallow-donor g factor.

	λ_{peak} [nm (eV)]	$g_{\|}$	$g_{\perp}$	$\|D\|$	$\|A_{\|}\|$ (10^{-4} cm^{-1})	$\|A_{\perp}\|$	$g_{\|}$(Cu) (calc.)	$g_{\perp}$(Cu) (calc.)
c-axis symmetry								
Type I	719 (1.72)	2.002		961	33		2.216	
Type II A	675 (1.83)	2.001	1.851	669	34	<7	2.214	1.930
Type II B	688 (1.80)	1.998	1.872	588	33		2.208	1.971
109°-axis symmetry								
Type III				1120				
Type IV A		2.001		695	33		2.228	
Type IV B		1.986	1.874	487	29		2.198	1.976
Type V A	708 (1.75)	1.981	1.880	379	10		2.188	1.988
Type V B	680 (1.82)	1.967	1.886	313	<4		2.160	2.000

modulation. Furthermore, as the c axis is rotated away from the magnetic field direction, the intensity of the high-field signal decreases rapidly and becomes negative (i.e., it corresponds to a decrease in emission intensity) at angles greater than 5°. The intensity of the low-field signal decreases less rapidly and always remains positive. Neither signal is observable at angles greater than ~20°.

Both the low- (Fig. 3) and high-field signals have a complex, asymmetric shape. With the magnetic field parallel to the c axis, the high-field signal is the mirror image of the low-field one except for an amplitude difference (see Fig. 2). To account for the overall shape of these signals, we propose that they are the superposition of the spectra of $S=1$ centers, all with the same g factor, but with a range of slightly differing values of the zero-field-splitting parameters. The spectral-dependence data discussed in Sec. V provide further evidence that we are dealing with a distribution of centers.

The structure which is partly resolved at the peaks of the broad type-I signals (Figs. 2 and 3) corresponds to a hyperfine interaction of about 33×10^{-4} cm^{-1}. The structure is associated with the type-I signals and is not due to a different type of spectrum accidentally superimposed. Its presence indicates that the distribution of zero-field-splitting parameters must be sharply peaked; that is, a large number of centers must have very similar D values. In applying the axial spin Hamiltonian of Eq. (1), we have used the centers of the hyperfine patterns to determine $g_{\|}$ and D, whose values are given, together with that of $A_{\|}$, in Table I. Because of the disappearance of the signals away from the c axis, values of $g_{\perp}$ and $A_{\perp}$ could not be determined.

B. Centers with symmetry axes at 109°

The other major lines in our ODMR spectra correspond to five more $S=1$ centers, which we shall label III, IV A, IV B, V A, and V B in order of decreasing zero-field splitting. The spin Hamiltonians for these centers are still approximately cylindrical, but their z axes are now inclined at 109°±3° to the c axis. These inclined z axes lie in the {1120} planes (or so close to these planes that we cannot tell the difference). Thus, they lie close to the Cd—S bond directions that are inclined at 107.4° to the c axis.

Since each type of center can be orientated in the lattice in six magnetically nonequivalent ways (or more if the symmetry is not exactly C_s), the ODMR spectra are, in general, extremely complex. Figure 5 shows a spectrum taken with B along the 109° direction, while a spectrum with B perpendicular to this direction in the (0001) plane is shown in Fig. 6. In Fig. 5 we can distinguish four pairs of low-field—high-field transitions corresponding to those sites of centers IV A, IV B, V A, and V B that have their z axes parallel to B. The type-III spectrum, not visible in Figs. 5 and 6, appears at higher pulse repetition rate and has larger splitting (240 mT for B along the 109° direction) than the type-IV A, -IV B, -V A, and -V B spectra.

For none of these centers have we been able to identify the lines for enough orientations to deduce the parameters of the true orthorhombic spin Hamiltonians. Therefore, and because our available data show that Eq. (1) is a good approximation, we give our results in a form that assumes $\tilde{g}$, $\tilde{A}$, and zero-field-splitting tensors with cylindrical symmetry about a 109° direction. In Table I the parameters $g_{\|}$, $A_{\|}$, and D come from measurements with B set at 109° to the c axis in a {1120} plane, and $g_{\perp}$ comes from

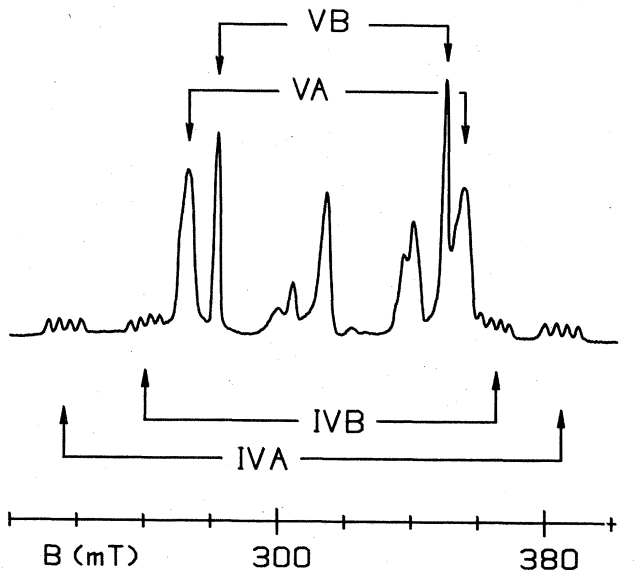

FIG. 5. ODMR spectrum at 2 K and 8.7 GHz for 514-nm excitation with the field at 109° to the c axis in a {1120} plane. The pulse sequence was as in Fig. 2 with a laser-pulse rate of 2.5 kHz. The labels indicate lines for sites of type-IV and -V centers having their z axes along the field for this orientation. The unlabeled lines in the central region correspond to other sites of these centers.

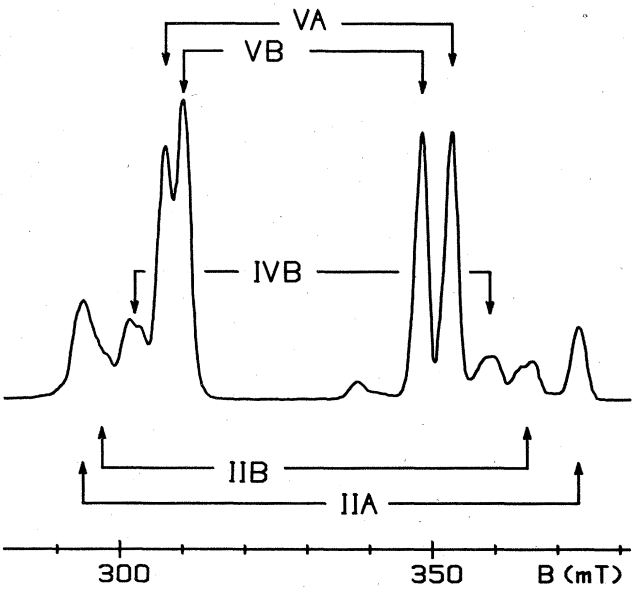

FIG. 6. ODMR spectrum as in Fig. 5, but with the field perpendicular to the c axis in a {1100} plane. The labels indicate lines for sites of type-IV B, -V A, and -V B centers having their z axes perpendicular to the field. The type-II A and -II B lines, not visible in Fig. 5, have reappeared in this orientation.

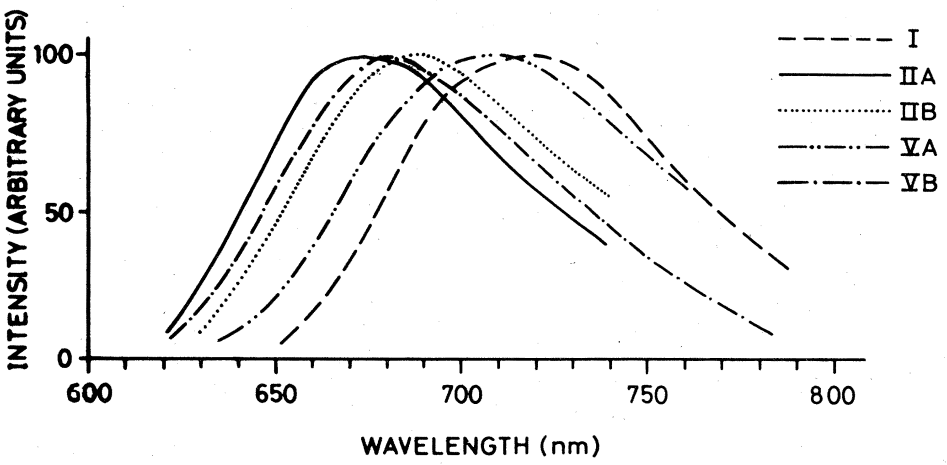

FIG. 7. Dependences of the ODMR signal intensities on emission wavelength for the type-I, -II A, -II B, -V A, and -V B spectra. The curves have been corrected for instrumental response and are expressed as changes in emission intensity per unit wavelength interval, normalized to the same maximum height in each case. They are to be compared with the emission spectrum of the same sample (Fig. 1). All data were obtained at 2 K and 8.7 GHz with 514-nm excitation.

measurements with B perpendicular to this direction in the (0001) plane.

Some of these spectra appear analogous to the spectra described in Sec. IV A. In particular, except for the different orientation of the z axis, the type-III spectrum is in several ways strikingly similar to the type-I spectrum: firstly, the type-III spectrum requires high pulse repetition rates to be observed; secondly, the lines are very broad (27 mT at half height); and thirdly, they disappear very quickly when B is rotated away from the z axis, being undetectable $\pm 3°$ away from the 109° direction.

The type-IV spectra resemble the type-II spectra in that they have well-resolved hyperfine splittings of order 3 mT (see Fig. 5). The type-IV A spectrum disappears if B is rotated more than $\pm 10°$ away from the 109° direction. The type-IV B spectrum can be followed over a wider range until it becomes lost among other lines; it appears again in spectra with B set perpendicular to the z axis (see Fig. 6). We note also that the spin-Hamiltonian parameters of the type-III and -IV spectra are very similar to those of the type-I and -II spectra (see Table I).

The type-V A and -V B spectra do not appear to have any c-axis—symmetry counterparts. In particular, these lines show no resolved hyperfine structure and the zero-field splittings are small (see Figs. 5 and 6, and Table I). These lines can be followed over most field orientations, disappearing only when the magnetic field makes an angle of between 45° and 65° with the z axis. The type-V A lines have strongly-orientation-dependent widths. We attribute this to an unresolved hyperfine interaction and (assuming $I=\frac{3}{2}$) deduce an approximate value for $|A_{\parallel}|$ (Table I). The type-V B lines are narrow at all field orientations.

V. DEPENDENCE OF ODMR INTENSITY ON EMISSION WAVELENGTH

The manner in which each of the five strongest types of ODMR spectra depends on the emission wavelength is shown in Fig. 7. The diagrams were obtained by interposing a monochromator between the sample and the photomultiplier, and measuring the peak intensity of each ODMR spectrum as a function of emission wavelength. The dependences of the type-I, -II A, -II B, -V A, and -V B ODMR signals have their maxima at wavelengths of (719±5) nm (1.72 eV), (675±5) nm (1.83 eV), (688±5) nm (1.80 eV), (708±5) nm (1.75 eV), and (680±5) nm (1.82 eV), respectively. We have been unable to obtain accurate values for the maxima for the weaker type-III, -IV A, and -IV B spectra, but use of color filters shows that these are also associated with the red-infrared band.

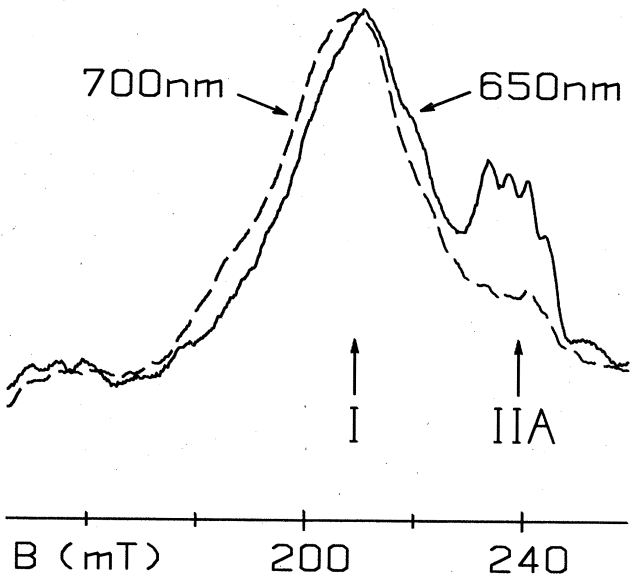

FIG. 8. Type-I low-field ODMR line as in Fig. 3 (but with higher microwave power, which reduces the resolution of the hyperfine structure. A monochromator restricts the monitored emission to an 1.8-nm band centered at 650 nm (solid curve) and 700 nm (dashed curve). The small shift observed corresponds to an increase in the zero-field-splitting parameter $|D|$ with increasing wavelength.

Experiments were also carried out to distinguish between the different parts of the distribution of centers that are responsible for the broad type-I ODMR spectrum. In Fig. 8 we show two type-I spectra, one recorded at an emission wavelength of 650 nm and the other at 700 nm. There is a small but reproducible shift in the ODMR spectrum corresponding to an increase in $|D|$ of about 25×10^4 cm^{-1}. The observation of this shift is strong evidence for the existence of the postulated range of centers for the type-I spectra.

VI. DISCUSSION

A. Exchange-coupled model

We begin with the type-II A spectrum, which is the best characterized. The hyperfine structure shown in Figs. 2–4 immediately suggests a center involving copper, a common impurity in II-VI semiconductors. This attribution is confirmed by the consideration of the g values given later. There are two naturally occurring copper isotopes, both with $I=\frac{3}{2}$ (^{63}Cu, 69% abundant; ^{65}Cu, 35% abundant); the slight difference in nuclear magnetic moments ($^{63}\mu$:$^{65}\mu=0.933$) is too small to be resolved in the present experiments. The hyperfine interaction of the type-II A centers is in the range characteristic of copper in the $3d^9$ configuration in II-VI materials.[21–23] For CdS, the EPR spectra of three such centers have been reported (with $S=\frac{1}{2}$), as summarized in Table II.

Table II also gives the g values for shallow donors with $S=\frac{1}{2}$ in CdS.[13] It is at once apparent (Tables I and II) that the value of $g_{\parallel}$ for the type-II A center is very close to the mean of $g_{\parallel}$ for the copper center reported by Schulz[23] and $g_{\parallel}$ for a shallow-donor center; the same is true for the values of $g_{\perp}$. This key feature leads us to conclude that the type-II A centers are exchange-coupled pairs, each consisting of a shallow-donor electron and the copper center reported by Schulz.

The spin Hamiltonian appropriate to an exchange-coupled pair can be written as[24,25]

$$\mathcal{H}_p=J\vec{S}_1\cdot\vec{S}_2+D_e(3S_{1z}S_{2z}-\vec{S}_1\cdot\vec{S}_2)+E_e(S_{1x}S_{2x}-S_{1y}S_{2y})+\beta\vec{B}\cdot\tilde{g}_1\cdot\vec{S}_1+\beta\vec{B}\cdot\tilde{g}_2\cdot\vec{S}_2+\vec{S}_1\cdot\tilde{A}_1\cdot\vec{I}_1\,,$$

where the subscript 1 refers to the copper center and the subscript 2 refers to the donor electron. The first term represents the isotropic component of the exchange interaction, while D_e and E_e represent the anisotropic components which arise because of spin-orbit coupling (magnetic dipole-dipole interactions between the two spins are also contained in D_e and E_e). For axial symmetry, $E_e=0$. Hyperfine interaction between the spin I_1 of the copper nucleus and the spin S_2 of the donor electron is assumed to be small and is not included in this equation.

When J is large compared with the other terms, the combined spin states form a singlet ($S=0$, where $\vec{S}=\vec{S}_1+\vec{S}_2$) and a triplet ($S=1$). Within the triplet, the effective spin Hamiltonian becomes

$$\mathcal{H}_T=D[S_z^2-\tfrac{1}{3}S(S+1)]+E(S_x^2-S_y^2)+\beta\vec{B}\cdot\tilde{g}\cdot\vec{S}+\vec{S}\cdot\tilde{A}\cdot\vec{I}_1\,,$$

where $\tilde{g}=(\tilde{g}_1+\tilde{g}_2)/2$, $\tilde{A}=\tilde{A}_1/2$, $D=D_e/2$, and $E=E_e/2$, provided that terms of the form $[(g_1-g_2)\beta B]^2/J$, which mix the singlet and triplet states, are small.[24,25] At 23 GHz this requires $|J|\gg0.3$ cm^{-1}. It is the spin Hamiltonian $\mathcal{H}_T$ (with $E=0$) that describes the type-II A ODMR spectrum.

We have already noted that the observed g tensor for the type-II A centers is the mean of those for shallow-donor electrons and Schulz-type copper centers. The components of $\tilde{A}$ should, as a first approximation, be equal to half of the values observed for the copper center when isolated. The value of $A_{\parallel}$ is indeed about one-half of the value of $A_{\parallel}$ observed by Schulz (Table II). The value of $A_{\perp}$ has not been determined, but the linewidth of the type-II A spectrum in the perpendicular orientation sets an upper limit to this quantity that is consistent with half of the value of $A_{\perp}$ obtained by Schulz.[23] The values of the hyperfine interaction thus strengthen the conclusion that the type-II A centers are exchange-coupled pairs consisting of a shallow-donor electron and the axial copper center of Schulz.[23]

The energy-level scheme for an $S=1$ axially symmetric center such as type II A is shown in Fig. 9 (B parallel to z). For ODMR to be observed the emission transition probabilities R_1 and R_0 must differ. For example, for a large singlet-triplet splitting [relative to $(g_1-g_2)\beta B$], one

TABLE II. Spin-Hamiltonian parameters for some $S=\frac{1}{2}$ centers in CdS. The mean values calculated in the last line are to be compared with data for the c-axis–symmetry $S=1$ centers (Table I).

	$g_{\parallel}$	$g_{\perp}$	$\lvert A_{\parallel}\rvert$ (10^{-4} cm^{-1})	$\lvert A_{\perp}\rvert$ (10^{-4} cm^{-1})
Cu-A[a]	2.240 ±0.005	1.75 ±0.05	105 ±5	28
Cu-B[a]	1.93	2.14	21	
Cu[b]	2.2206±0.0005	1.924 ±0.002	77.2±0.2	23±10
D[c]	1.7877±0.0005	1.7720±0.0007		
Mean of D[c] and Cu[b]	2.0043±0.0005	1.844 ±0.002	38.6±0.1	12±5

[a] Morigaki, Ref. 22.
[b] Schulz, Ref. 23.
[c] Shallow donor, Ref. 13.

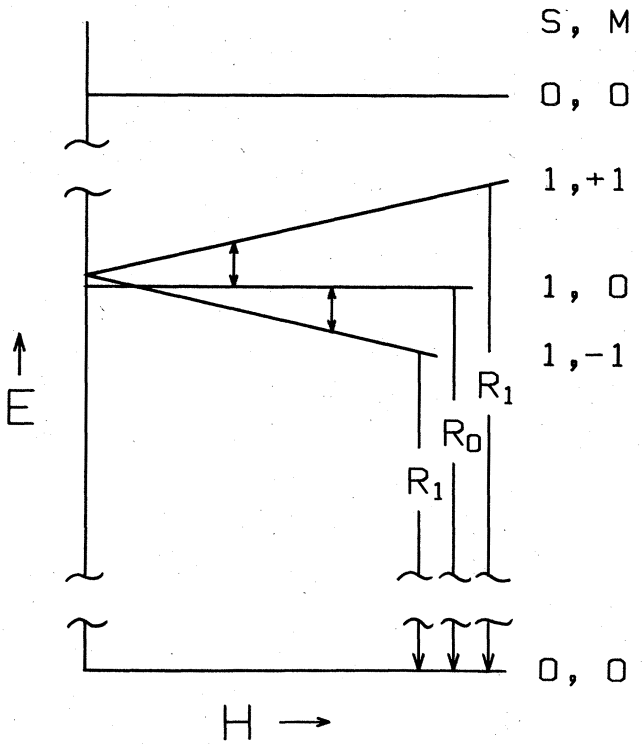

FIG. 9. Energy—versus—magnetic-field diagram for a copper-center—donor pair. The diagram is drawn for the case of strictly axial symmetry with the field along the z axis. In the excited state, combination of the two spins $S=\frac{1}{2}$ produces a triplet $S=1$ and a singlet $S=0$. The singlet is taken arbitrarily to have the higher energy, and the zero-field splitting of the triplet, D, is taken to be positive. R_0 and R_1 are the transition probabilities for the indicated optical transitions to the singlet ground state. The allowed microwave transitions ($\Delta M=\pm 1$) within the triplet are also shown.

expects $R_1 \gg R_0$, and, if spin relaxation is slow, the population in $|0\rangle$ will exceed that in $|\pm 1\rangle$. At resonance, microwave transitions will transfer spin from the slowly emitting state $|0\rangle$ to the more quickly emitting states $|\pm 1\rangle$, and increases in emission will be observed. A similar situation is encountered if $R_0 \gg R_1$, as expected for a small singlet-triplet splitting: Our present data cannot distinguish which of the two situations applies.

As the magnetic field is rotated away from the c axis, mixing among the triplet states occurs and the differences in emissive-transition probabilities become less marked. The ODMR signal intensities are expected to decrease gradually, as is indeed observed for the type-II A centers. This behavior is typical of ODMR spectra from triplet states in strictly axial symmetry.[5,7]

The spin-Hamiltonian parameters for the type-I and -II B spectra are similar to those of the type-II A spectra, and this strongly suggests that pairs consisting of shallow-donor electrons and Schulz-type copper centers are again involved. To account for the differences between the type-II A and the other spectra, it is necessary to assume that the relative positions of the donor and copper center are different in each type of pair. The symmetry of the type-I and -II B spectra is almost certainly lower than axial. While we have no *direct* evidence that this is so for the type-I spectra, it would be extremely difficult to account for the range of pairs required to give the distribution of D values observed for these signals if all such pairs were required to have axial symmetry. A marked difference between the behavior of the type-I and -II A spectra is the very rapid decrease in intensity of the type-I signals as the field direction is rotated away from the c axis, and the eventual reversal in sign of the high-field component. This reversal appears to signify a population distribution dominated by thermalization within the triplet sublevels rather than a distribution dominated by a difference between the recombination probabilities R_0 and R_1. The thermalization appears to be more effective for field directions away from the c axis. We do not understand this behavior at present, but it may be associated with additional mixing of the pair states by low-symmetry terms in the Hamiltonian.

For the type-II B pairs, we have already noted (Sec. IV) the possible existence of low-symmetry terms in the spin Hamiltonian, and these may account for the disappearance of these signals at field angles of greater than 15° to the c axis.

A model in which a shallow-donor electron is strongly coupled to a hole in the $3d$ shell of the copper center reported by Schulz thus accounts well for the spin-Hamiltonian parameters obtained for the type-I, -II A, and -II B ODMR spectra. The similarity between these c-axis centers and the centers with z axes at 109° to the c axis means that the latter centers can almost certainly be explained within the same framework of the strongly-coupled—pair model. We assume that the donor-electron radius is so large that the electron density is practically constant over the region occupied by the highly localized hole. Then the anisotropic component of the electron-hole—exchange interaction, due mainly to the copper-ion spin-orbit coupling, should have essentially cylindrical symmetry with its axis along that of the copper center, the position of the donor having only a relatively small effect. Thus, for the type-III, -IV A, -IV B, -V A, and -V B pairs the copper center that is coupled to the donor must itself have its symmetry axis along the 109° direction; as before, we presume that the relative positions of the donor and the copper center are different for each type of pair. Within this framework the g values of the copper centers themselves can be deduced from the pair g values given in Table I and the g values of the donor electrons given in Table II by means of the expression $2g(\text{pair})-g(\text{donor})$. These values are given in Table I.

B. Nature of the $S=\frac{1}{2}$ copper centers

A major question posed by Schulz's EPR work is whether the copper ion in axial symmetry is isolated or associated with another impurity or defect. For *cubic* II-VI compounds, convincing arguments for the impossibility of observing magnetic resonance from isolated substitutional Cu^{2+} ions because of the strong spin-lattice coupling have been put forward by the Clerjaud and Gélineau.[26] However, in wurtzite-structure compounds there is a trigonal crystal field to reduce the orbital degen-

eracy, and the EPR of isolated Cu^{2+} appears definitely to have been identified in ZnO (Ref. 27) and possibly in hexagonal ZnS (Refs. 21 and 28) and in BeO (Ref. 29).

Schulz's center has the proper symmetry to be an isolated Cu^{2+} ion, but at least two other trigonal-symmetry centers are known in CdS (see Table II). Of the three centers, it is Morigaki's B center that is the best candidate to be an isolated Cu^{2+}: This center has $g_{\|} < g_{\perp}$ as in the above-mentioned centers in ZnO, ZnS, and BeO. In contrast, Schulz's center has $g_{\|} > g_{\perp}$. The latter ordering of the g values suggests a very different crystal field, one that might be produced by another defect situated along the c axis from the Cu^{2+} ion. Moreover, in Schulz's published EPR spectrum[23] and in figures given in Ref. 30 there appear other resonances which are due to copper ions in lower symmetry. Schulz did not analyze these spectra, but at least some of them must be due to the formation of associates.

Our ODMR work provides further evidence for association effects. For example, for the type-IV A pairs, the center that is coupled to the donor is deduced to have g factors and hyperfine interactions very close to those of Schulz's center, but with the major axis (z axis) inclined at 109° to the c axis. This is surely just a different geometrical configuration of the same basic center. One possible explanation is that these different configurations correspond to static trigonal Jahn-Teller distortions; however, there is much evidence from data for transition-metal ions in other tetrahedral surroundings that t_2-symmetry d orbitals interact strongly only with tetragonal distortions of the coordination tetrahedron.[31] We therefore conclude that the copper centers are associate centers.

We are thus led to propose that all of the $S=\frac{1}{2}$ centers consist of substitutional Cu^{2+} ions, each associated with an impurity or defect X in the near vicinity. In some cases X lies on the c axis passing through the copper ion, thus giving Schulz's center, while in other cases the symmetry properties suggest that it lies near a 109° direction. The obvious position for X is then one of the four sulfur sites nearest the copper ion. In the CdS structure one bond direction lies along the c axis, while the other three are directed at 107.4° to this axis. Because of the proximity of defect X to the copper ion, the principal axis of the g tensor will lie close to the appropriate Cu—X bond direction. Likely possibilities for X are halogen impurities, with charge $Q=1$ relative to the lattice, or chalcogen impurities (e.g., oxygen), with $Q=0$.

C. Pair configurations

The pair model that we consider is one in which the CuX associate lies close to a donor, as represented in Fig. 10(a). We assign our different ODMR spectra to different configurations of the donor-CuX pairs, and discuss if the different emission wavelengths observed in Fig. 7 are consistent with this model.

In the *excited* state (i.e., before emission) the shallow-donor electron is exchange-coupled to the hole in the copper $3d$ shell, the copper being in the divalent $3d^9$ state, that is, neutral with respect to the lattice. In the *final* state (after emission), the electron has annihilated the hole, giving a singlet ground state, as represented in Fig. 9. The copper is now in the monovalent $3d^{10}$ state, that is, negatively charged with respect to the lattice. We assume that the separation between the donor impurity and the CuX associate is small in comparison with the dimensions of the orbital occupied by the electron, as represented schematically in Fig. 10. We also assume that the donor impurity does not occupy one of the nearest-neighbor sulfur sites to the copper ion since the simultaneous presence of X and D in this shell would result in centers of symmetry different from those observed.

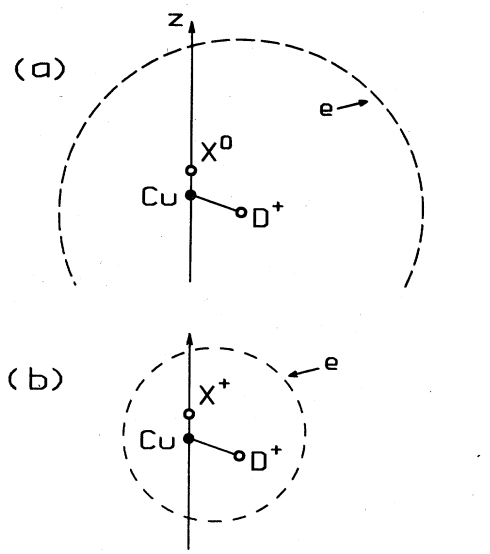

FIG. 10. Two possible models for the $S=1$ centers described in this paper. Donor core D^+ lies near a neutral copper acceptor Cu. An unidentified defect X occupies the sulfur site along the z direction from the Cu acceptor (z is the c axis for type-I and -II centers; z is the 109° axis for type-III, -IV, and -V centers). In model (a), X is neutral and the electron orbital is centered on D^+. In model (b), X is charged and the electron is trapped in a smaller-radius orbital by the combined fields of D^+ and X^+. Recombination of the electron with the acceptor hole produces the visible-red-infrared luminescence. All the charges are expressed relative to the normal charges at the corresponding lattice points.

Because of the Coulomb interaction between the positively charged donor core D^+ and the monovalent copper in the final state, the expression for the emission energy contains a term of the form[11]

$$E_c=(e^2/4\pi\epsilon_0 r)(\epsilon_{\|}\epsilon_{\perp}\sin^2\theta+\epsilon_{\perp}^2\cos^2\theta)^{-1/2}\,, \tag{2}$$

where r and θ represent the polar coordinates of D^+ with respect to the copper ion.

If the effective charge Q of impurity X is zero, this is the only significant distance-dependent term in the emission energy. If $Q=+1$, the problem is slightly more complicated. The electron will now be bound to the *pair* of cores D^+ and X^+ [Fig. 10(b)] and its binding energy will depend on the separation of D^+ and X^+. If the effective-mass model remains valid (and we assume this is so, for the electron g factor deduced in Sec. VI A is characteristic of a *shallowly* bound electron), the energy

involved here is not very large. For small separation of X^+ and D^+, the combination of these two charges will act as a double-donor core, binding a single electron by, at most, $4E_D$, where E_D is the single-donor binding energy of about 30 meV.[32,33] The radius of the orbital occupied by the electron will then be half of the single-donor radius, that is, taking $a_D=3.0$ nm,[33] about 1.5 nm. We expect the electron binding energy to be relatively insensitive to the exact positions of X^+ and D^+ as long as their separation is much less than this distance. The Coulomb term will therefore still be the only significant distance-dependent term in the expression for the emission energy.

We have calculated E_c for the possible values of r and θ in the CdS structure, using $\epsilon_{||}=9.00$ and $\epsilon_{\perp}=8.37$;[34] some values are given in Table III. These values are subject to uncertainty: Firstly, because the values of $\epsilon_{||}$ and $\epsilon_{\perp}$ are known only to within $\pm 2\%$;[34] secondly, because the concept of a macroscopic dielectric constant may not be valid at small values of r; and thirdly, because the environment of the impurities may be significantly distorted from the idealized lattice configuration. For all these reasons the values given in Table III will be considered only as a rough guide as to whether or not it is possible to account for the spread in emission energies associated with the different pairs.

TABLE III. Coulomb interactions between a charge $-|e|$ on a cadmium site at the origin and a charge $+|e|$ on neighboring sites at positions r and θ in the CdS structure; n is the number of equivalent sites. The calculation uses the macroscopic dielectric constants $\epsilon_{||}=9.00$ and $\epsilon_{\perp}=8.37$ (Ref. 34), and the values $a=0.414$ nm, $c=0.671$ nm, and $u=0.261$ nm for the CdS lattice parameters [Joint Committee on Powder Diffraction Standards File No. 6-0314 (International Center for Diffraction Data, Swarthmore, Pennsylvania, 1982)]. All pairs of sites are listed out to 0.827 nm separation. In our model the copper ion occupies the central cadmium site, defect X occupies one of the first-neighbor sulfur sites (first two lines of table), and donor core D^+ occupies various sites in the next few shells.

r (nm)	θ (deg)	E (meV)	n
	(a) Charge $+\|e\|$ at sulfur sites		
0.250[a]	107.4	665	3
0.261[a]	0	659	1
0.410	180	419	1
0.483	98.9	344	3
0.489	57.7	343	6
0.583	134.8	290	6
0.643	21.8	266	3
0.636	96.7	261	6
0.764	38.7	222	3
0.783	162.2	219	3
0.762	70.0	218	6
0.826	119.8	203	6
	(b) Charge $+\|e\|$ at cadmium sites		
0.412	35.4, 144.6	412	3, 3
0.414	90	401	6
0.584	54.9, 125.1	288	3, 3
0.671	0, 180	256	1, 1
0.715	62.0, 118.0	234	6, 6
0.716	90	232	6
0.788	31.6, 148.4	216	6, 6
0.827	90	201	6

[a] It is assumed that D^+ cannot occupy these positions and these two rows are given for completeness only.

The type-II A center has the highest emission energy and is of strictly axial symmetry. A possible model for this center is thus one in which the donor D lies at the position (0.410 nm, 180°) relative to the Schulz CuX associate (for which we recall that the Cu-X axis is itself along the c axis). Models for the other c-axis pairs (type-II B and the range of type-I centers) would then involve placing the donor at other nearby sulfur sites (the Cu-X axis still being along the c axis). The data of Table III(a) show that the Coulomb shifts when the donor is placed at different sulfur sites differ by amounts which are of the order of the 0.11-eV spread in the emission-energy dependences of the ODMR spectra. The configuration postulated above for the type-II A center is at highest energy, as required, although for the reasons discussed in the preceding paragraph we cannot expect better than order-of-magnitude agreement between the observed and calculated shifts in emission wavelength between different types of pairs. A similar conclusion is arrived at for the 109° spectra; here the donors are envisaged to be placed at different values of r and θ relative to CuX associates whose axes are in bond directions other than [0001].

In Table III(b) are given the Coulomb energies corresponding to the donor D being placed at cadmium sites. In this case it is more difficult to account for the emission-energy dependences of the different ODMR signals: For example, the highest emission energy should correspond to a pair which does not have strictly axial symmetry about the c axis, and which could not therefore give the type-II A ODMR spectrum. The placing of the donors at sulfur sites therefore appears more likely.

D. Further discussion of the pair parameters

Many properties of the pairs remain unexplained and we review some of them in this section. We have not made any attempt to obtain theoretical values for the zero-field-splitting parameter D; any such calculation would be extremely complicated and the result is likely to depend not only on the intrapair separation but also on the pair orientation. The spectral-dependence data for the different types of centers (Table I) and the shift of the type-I ODMR line with emission wavelength (Fig. 8) show that, for both c-axis—symmetry spectra and 109°-direction—symmetry spectra, the zero-field splitting decreases with increasing optical energy (the only exception is the relative order of the type-II A and -II B centers). From the above discussion of Coulomb shifts, this implies that D decreases as the pair separation becomes smaller. We can offer no explanation of this puzzling point. Table I also highlights another interesting point, namely that as D becomes smaller, $g_{||}$ decreases while $g_{\perp}$ increases slightly; $A_{||}$ also decreases. This suggests that the model in which the parameters of the $S=1$ center are taken to be the average of the parameters for the relevant isolated $S=\frac{1}{2}$ centers is beginning to break down for the very closest separations. We have no explanation for this at

present, particularly because we lack a theory for the spin-Hamiltonian parameters of the copper centers. According to static crystal-field theory,[35] values of $|g_{\parallel}|$ slightly greater than 2 and of $|g_{\perp}|$ slightly less than 2 can only be obtained for trigonal-field-splitting parameters much smaller than the spin-orbit—coupling constant. This is inconsistent with a model of a copper ion strongly perturbed by an adjacent defect X. However, it is known that the magnetic properties of copper in trigonal symmetry can be profoundly modified by dynamic Jahn-Teller effects. The relevant theory has been applied in some detail to cases for which $g_{\perp} > g_{\parallel}$;[36,37] its extension to the opposite situation could help to explain our results. We note also that the Jahn-Teller effect may strongly influence the values of the zero-field-splitting parameter D since this involves the copper-center spin-orbit coupling.

VII. CONCLUSIONS

ODMR signals from eight types of spin-triplet systems have been observed for CdS. The type-II A spectrum shows well-resolved hyperfine structure due to copper nuclei and has axial symmetry. The parameters of the spin Hamiltonian are readily accounted for by attributing the spectrum to pairs each consisting of a shallow-donor electron strongly coupled to a hole in the $3d$ shell of the copper ion in the axial center that was previously reported by Schulz.[23] The values of $\tilde{g}$ and D for the type-I and -II B centers are similar to those of type II A, and similar pair models are also proposed for these spectra. The slight differences in spin-Hamiltonian parameters and the differences in optical emission energies are accounted for by geometrically different configurations of the pair. In a similar way the ODMR spectra with symmetry axes in the 109° directions are attributed to pairs formed by shallow-donor electrons and variants of the Schulz copper center in which the CuX axes are along bond directions other than [0001]. Again, different geometrical arrangements of the pair are assumed to be responsible for the range of spectra observed.

Several of the previously reported triplet-state ODMR signals in semiconductors have been for species that are analogous to those reported here.[4–7] These species have usually been referred to as bound excitons. This could also be considered an appropriate name for our strongly coupled electron-hole pairs, but we have preferred to emphasize a description in terms of the properties of a copper-center—donor pair in the limit of very small separation. This is because our results represent the first case in which the g factors and hyperfine parameters can be related directly to those of the individual $S = \frac{1}{2}$ centers from which the triplet is created.

In the early studies of II-VI—compound phosphors (see, e.g., the reviews in Ref. 38), electron-hole recombination at near-neighbor donor-acceptor pairs was a popular model for explaining many of the broad luminescence bands given by these materials. However, time-resolved luminescence measurements, and, more recently, a large number of ODMR studies, have shown that most of the well-known bands correspond to distant-pair electron-hole—recombination processes. The present work is the first case in any II-VI compound in which deep-center luminescence has been unambiguously identified as being due to recombination at close donor-acceptor pairs. The emission from CdS at 720 nm is remarkably intense, implying a high quantum efficiency for the process, even though the defects involved are accidental impurities. This suggests that recombination at close pairs could indeed be important in II-VI compounds. If the electron-hole states involved are spin triplets, as in the case we have studied in CdS, ODMR should prove to be the most useful technique for identifying such recombination processes.

ACKNOWLEDGMENTS

We are grateful to M. Moulin and G. Bastide for providing the CdS crystals used in this investigation, and to I. Broser, R. Broser, and M. Schulz for helpful discussions.

*Permanent address: Department of Physics, University of Hull, Hull HU6 7RX, United Kingdom.

[1]R. T. Cox, D. Block, A. Hervé, C. Santier, and R. Helbig, Solid State Commun. **25**, 77 (1978).
[2]J. E. Nicholls, J. J. Davies, B. C. Cavenett, J. R. James, and D. J. Dunstan, J. Phys. C **12**, 361 (1979).
[3]J. J. Davies and J. E. Nicholls, J. Phys. C **15**, 5321 (1982).
[4]P. Dawson, N. Killoran, and B. C. Cavenett, Solid State Commun. **32**, 1333 (1979).
[5]S. Depinna, B. C. Cavenett, N. Killoran, and B. Monemar, Phys. Rev. B **24**, 6740 (1981).
[6]N. Killoran, B. C. Cavenett, and F. Levy, Solid State Commun. **44**, 459 (1982).
[7]K. P. O'Donnell, K. M. Lee, and G. D. Watkins, Solid State Commun. **44**, 1015 (1982).
[8]M. Moulin, Rev. Tech. Thomson—CSF **1**, 365 (1969).
[9]Centre d'Etudes d'Electronique des Solides, Université des Sciences et Techniques de Languedoc, Montpellier, France.
[10]D. Block, A. Hervé, and R. T. Cox, Phys. Rev. B **25**, 6049 (1982).
[11]For example, C. H. Henry, R. A. Faulkner, and K. Nassau, Phys. Rev. **183**, 798 (1969).
[12]R. F. Brunwin, B. C. Cavenett, J. J. Davies, and J. E. Nicholls, Solid State Commun. **18**, 1283 (1976).
[13]J. L. Patel, J. E. Nicholls, and J. J. Davies, J. Phys. C **14**, 1339 (1981).
[14]For example, C. C. Klick, J. Opt. Soc. Am. **41**, 816 (1951).
[15]F. A. Kroger, H. J. Vink, and I. van den Boomgaard, Z. Phys. Chem. (Leipzig) **203**, 1 (1954).
[16]I. Broser and R. Broser-Warminsky, Z. Elektrochem. **61**, 79 (1957).
[17]I. Broser, R. Broser-Warminsky, and H. J. Schulz, in *Proceedings of the International Conference on Semiconductor Physics, Prague, 1960* (Academic, New York, 1961), p. 771.
[18]I. Broser, H. Maier, and H. J. Schulz, Phys. Rev. **140**, A2135 (1965).

[19]I. Broser (private communication).
[20]J. J. Davies, J. Phys. C **11**, 1907 (1978).
[21]W. C. Holton, M. de Wit, R. K. Watts, T. L. Estle, and J. Schneider, J. Phys. Chem. Solids **30**, 963 (1969).
[22]K. Morigaki, J. Phys. Soc. Jpn. **19**, 1240 (1964); in *II-VI Semiconducting Compounds,* proceedings of the 1967 International Conference, edited by D. G. Thomas (Benjamin, New York, 1967), p. 1348.
[23]M. Schulz, Solid State Commun. **11**, 1161 (1972).
[24]For example, J. Owen and E. A. Harris, in *Electron Paramagnetic Resonance,* edited by S. Geschwind (Plenum, London, 1972), Chap. 6.
[25]For example, J. Owen, in Proceedings of the Sixth Symposium on Magnetism and Magnetic Materials, New York, New York, 1960 [J. Appl. Phys. Suppl. **32**, 213 (1961)].
[26]B. Clerjaud and A. Gélineau, Phys. Rev. B **16**, 82 (1977).
[27]R. E. Dietz, H. Kamimura, M. D. Sturge, and A. Yariv, Phys. Rev. **132**, 1559 (1963).
[28]M. de Wit, Phys. Rev. **177**, 441 (1969).
[29]M. de Wit and A. R. Reinberg, Phys. Rev. **163**, 261 (1967).
[30]M. Schulz, doctoral dissertation, Universität, Berlin, 1971.
[31]For example, M. D. Sturge, in *Solid State Physics,* edited by F. Seitz, H. Ehrenreich, and D. Turnbull (Academic, New York, 1967), Vol. 20, p. 92.
[32]C. H. Henry and K. Nassau, Phys. Rev. B **2**, 997 (1970).
[33]M. Moroz, Y. Brada, and A. Honig, Solid State Commun. **47**, 115 (1983).
[34]A. S. Barker and C. J. Summers (unpublished), cited in Ref. 32.
[35]For example, A. Abragam and B. Bleaney, *Electron Paramagnetic Resonance of Transition Ions* (Oxford University Press, London, 1979), Chap. 7.
[36]C. A. Bates and P. E. Chandler, J. Phys. C **4**, 2713 (1971).
[37]T. Yamaguchi and H. Kamimura, J. Phys. Soc. Jpn. **33**, 953 (1972).
[38]*Physics and Chemistry of II-VI Compounds,* edited by M. Aven and J. S. Prener (North-Holland, Amsterdam, 1967).